

Conf-950846--1
SAND95-1191C

Abstract Submitted
for the American Physical Society
1995 Topical Conference on
Shock Compression of Condensed Matter
13-18 August 1995

Suggested title of session
in which paper should be placed:
Space Applications

Physics and Astronomy
Classification Scheme
Number 62.50

RECEIVED

JUN 19 1995

OSTI

Hypervelocity Impact Testing of Spacecraft Optical Sensors - J. S. BROWNING and J. L. MONTOYA, Sandia National Laboratories, -- Hypervelocity tests of spacecraft optical sensors were conducted to determine if the optical signature from an impact inside the optical sensor sunshade resembled signals that have been observed on-orbit. Impact tests were conducted in darkness and with the ejected debris illuminated. The tests were conducted at the Johnson Space Center Hypervelocity Impact Test Facility. The projectile masses and velocities that may be obtained at the facility are most representative of the hypervelocity particles thought to be responsible for a group of anomalous optical sensors responses that have been observed on-orbit. The projectiles are a few micrograms, slightly more massive than the microgram particles thought to be responsible for the signal source. The test velocities were typically 7.3 km/s, which are somewhat slower than typical space particles.

*This work performed at Sandia National Laboratories supported by the U. S. Department of Energy under contract DE-AC04-94AL85000.

Prefer standard session

L. C. Chhabildas, APS Member
Sandia National Laboratories
Department 1433, MS-0821
Albuquerque, NM 87185-0821



DISTRIBUTION OF THIS DOCUMENT IS UNLIMITED

MASTER

Background

History

The advent of orbiting space platforms in the early 1960's opened a whole new field of observing, monitoring and studying the Earth. Sandia National Laboratories have developed optical sensors to detect nuclear bursts. The development of nuclear detonation detection systems is a textbook case of the application of engineering knowledge to provide society with the goods and services needed to maintain an appropriate defense establishment.

However, some areas remain unsettled, and have never been treated adequately to satisfy intellectual curiosity. These sensors have the capacity to acquire information about physical quantities not perceived by human senses because of their subliminal nature. For example, the optical sensors are capable of observing light emitted from lightning, meteorites, and perhaps other unknown processes. The primary focus has been on deciding whether a recorded optical event is evidence of a nuclear burst. What other information may be present in the signals of unknown origin has essentially remained a matter of speculation.

Theory

In January of 1994 Dick Spalding (Senior Engineer for Exploratory Technology), Norm Blocker (Operational Satellite Payloads) and Gary Scrivner (Radiation and Electromagnetic Analysis Department) became interested in a theory of Craig Fox and Bob Wiley (Science Applications International Corporation) that a group of the unknown signals might be caused by hypervelocity microparticle impacts on the inside of the optical sensor sunshade [Fox and Wiley, 1994]. The frequency of the occurrence of the signals seemed to agree with the statistics associated with microgram-size orbital debris. However, the signal duration of several milliseconds and other characteristics were inconsistent with the optical signatures reported in the literature in a loosely defined field called "Cosmic Dust." The laboratory experiments indicated that the plasma from hypervelocity impacts lasts only tens of microseconds. The theory of Fox and Wiley was discounted by some because it was thought that the amount of light from a hypervelocity impact would not be detected by the optical sensor either because the light from the impact would be too dim to be detected, or that the baffles in the sunshade would block the light from reaching the optical detector.

Charlie Vittitoe (Optics and Exploratory Technologies) analyzed the impact scenario proposed by Fox and Wiley, and suggested the idea that the signal from the optical detector may not be caused by light emission from the expanding plasma cloud, but instead may be the result of sunlit

DISCLAIMER

**Portions of this document may be illegible
in electronic image products. Images are
produced from the best available original
document.**

ejecta. Clues included a characteristic inverse square time decay at late times in some signals and the signal magnitudes. Based upon these considerations a testing sequence for the purpose of observing the spacecraft optical sensor response to hypervelocity impacts on the sunshade was developed. The following were established as the test conditions:

- line-of-sight view of the impact site by the spacecraft optical sensor
- impacts inside the sunshade in darkness
- impacts inside the sunshade with the ejected debris illuminated

DISCLAIMER

This report was prepared as an account of work sponsored by an agency of the United States Government. Neither the United States Government nor any agency thereof, nor any of their employees, makes any warranty, express or implied, or assumes any legal liability or responsibility for the accuracy, completeness, or usefulness of any information, apparatus, product, or process disclosed, or represents that its use would not infringe privately owned rights. Reference herein to any specific commercial product, process, or service by trade name, trademark, manufacturer, or otherwise does not necessarily constitute or imply its endorsement, recommendation, or favoring by the United States Government or any agency thereof. The views and opinions of authors expressed herein do not necessarily state or reflect those of the United States Government or any agency thereof.

(A)
DISTRIBUTION OF THIS DOCUMENT IS UNLIMITED

Test Execution

Gas Gun Operation

Figure 1 is a schematic of the JSC HIT-F two-stage gas gun. The operation of the gun begins with the percussion firing of a few grams of powder in a shotgun shell. The burning powder propels a plastic piston that compresses hydrogen gas. Shown in Figure 1 at about the center of the gun, the piston reaches a stop where an aluminized mylar membrane is located. The membrane bursts, and the compressed hydrogen gas is released into the rifle barrel. The compressed gas propels a sabot down the barrel. The sabot is machined from a cylindrical piece of nylatron that is cut along its axis into four wedge-shape sections. An aluminum projectile, with a mass of a few micrograms, is contained in a small cavity drilled into the axis of the sabot. The rifle barrel imparts a spin to the sabot. When the sabot reaches the end of the barrel, the four sections separate and impact an aluminum plate called a "sabot catcher." The aluminum projectile passes unimpeded through a small hole in the sabot catcher and enters the test chamber. The muzzle velocity of the aluminum projectile is typically 7.3 km/s.

A comparison of the sizes of an aluminum projectile and a grain of salt is shown in Figure 2. The diameter of the projectile is 0.13 micrometers, about a fifth of the length of the diagonal of the grain of salt.

Preparation

In Figures 3 and 4 the setups for line-of-sight tests and the dark and illuminated debris tests are shown. All of the tests were conducted in a large, steel vacuum chamber 60 inches in length with a diameter of 44 inches. The chamber has a large rear door and two smaller doors on each side that permit access to the chamber. The chamber vacuum of about 400 microtorr was achieved by a large piston pump.

For the line-of-sight tests a target disk of sunshade material was located on a mounting fixture attached to the rear door of the test chamber. The target disk was centered on the axis of the chamber. The spacecraft optical sensor ("BDY Sensor"), without the sunshade attached, was located off-axis and resting on the floor of the chamber near the projectile entrance port. The optical sensor had a line-of-sight view of projectile impacts on the target disk. The test setup is shown in Figure 3.

For the dark and debris illuminated tests the spacecraft optical sensor, with the sunshade attached, was located approximately in the center of the test

chamber, as shown in Figure 4. The spacecraft optical sensor ("BDY, Sensor") was tilted at an angle of 34 degrees from the floor of the chamber, viewed a black cloth background, and did not have a line-of-sight view into the projectile entrance port. Dark green blotter paper was taped on the chamber walls to minimize any reflections of light emitted by projectile impacts, sabot impacts or from the muzzle. The projectile target was the sunshade. The projectile impacted on the third baffle from the lens of the optical sensor. In this setup the spacecraft optical sensor did not have a line-of-sight view of the impact site. A second optical detector ("BDY Diode") was located near the rim of the sunshade with a line-of-sight view of the impact site. A 1.5 million candle spotlight, with a halogen bulb, was located on the floor of the chamber to illuminate debris ejected out of the sunshade. The spotlight was powered by a rechargeable lead-acid battery. All unused ports to the chamber were sealed to block out light from the outside of the chamber. A set of three baffles with 1 inch diameter apertures was positioned between the sabot catcher and the projectile entrance port to minimize the light entering the chamber from the gas gun. For the dark tests, referred to in this report as "tests in darkness," the spotlight was turned off. For the illuminated debris tests the spotlight was turned on. The test setup is shown in Figure 4.

Instrumentation

Two optical detectors were used in the hypervelocity impact tests. Both of the optical detectors used silicon photodiodes which detect light between the wavelengths of 0.4 and 1.1 microns with a peak sensitivity at 0.9 microns. One of the optical detectors, used in all of the tests, was the silicon photodiode and the signal conditioning portion of a spacecraft optical sensor. The fast response of the photodiode is amplified by a chain of amplifiers. The desired gain may be selected by tapping into the appropriate signal node along the chain. The slow response of the photodiode is canceled by a feedback circuit which uses a time average of the photodiode response.

The second optical detector consisted of a silicon photodiode and signal conditioning electronics similar in function, but not identical to the spacecraft optical sensor.

Prior to using the optical detectors at the JSC HIT-F, both detectors were tested at Sandia with various light sources in order to understand the limitations and characteristics. The performance of the detectors was compared to other available optical detectors to examine bandwidth characteristics (i.e., risetime and falltime, linearity, sensitivity and saturation characteristics). From the recorded data, of significance was the fact that the satellite optical sensor had a risetime (and falltime) of 18 microseconds,

and the other optical detector used at the JSC HIT-F had a time constant of approximately 60 microseconds (see Appendix).

In order to confirm the proper functioning of the detectors and the data recording instrumentation prior to each shot of the JSC HIT-F gas gun, a small strobe light was used as a reference light source. The recorded signature from this source confirmed that each of the detectors was functioning properly at shot time.

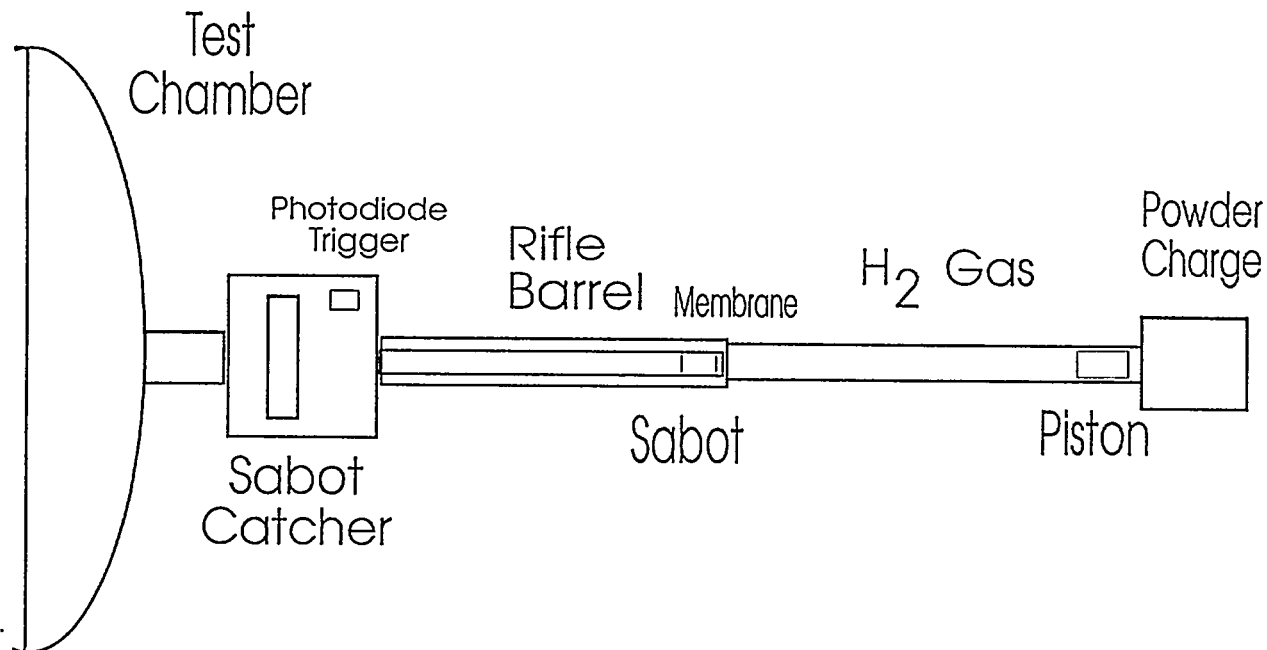


Figure 1. JSC HIT-F Two Stage Gas Gun

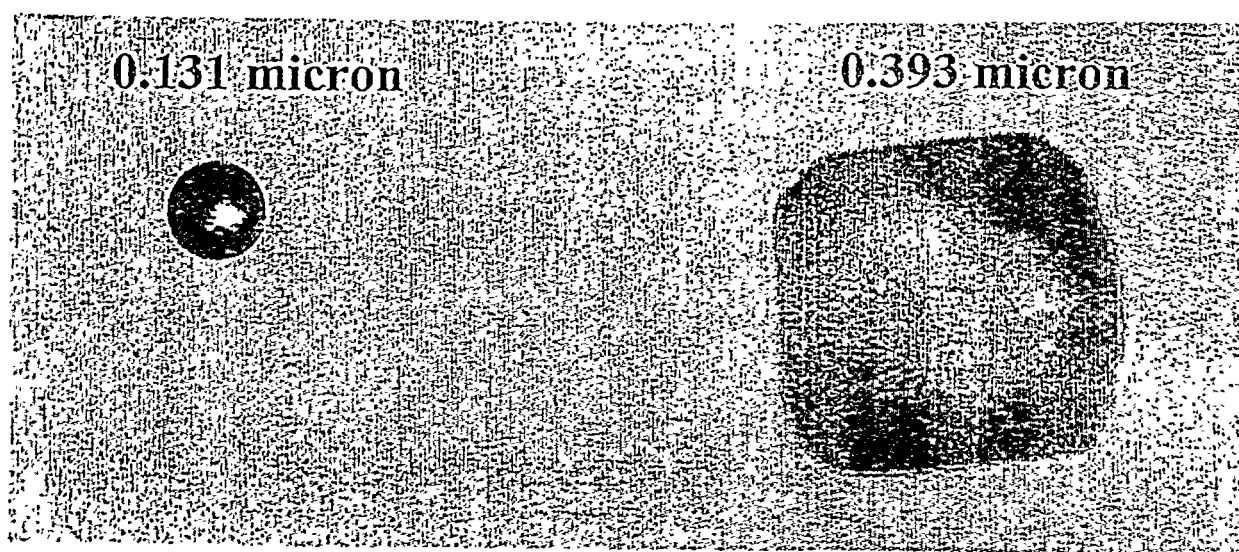


Figure 2. Aluminum Projectile (left) and Grain of Salt (right)

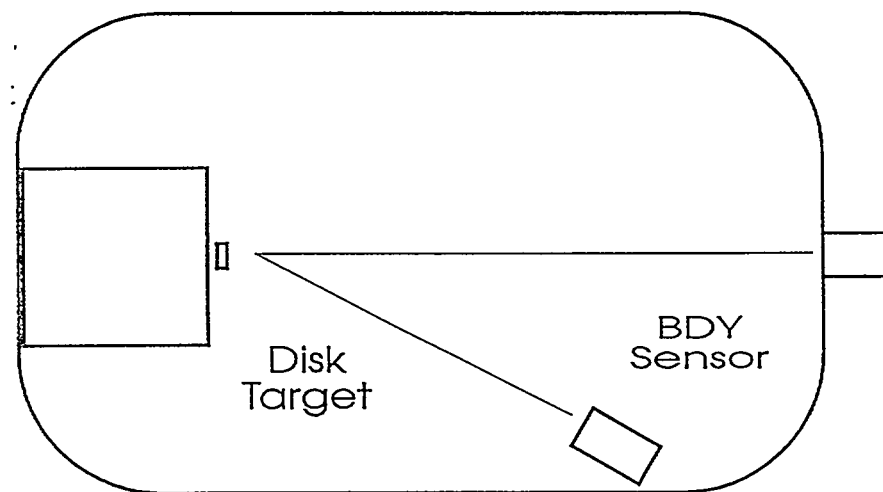
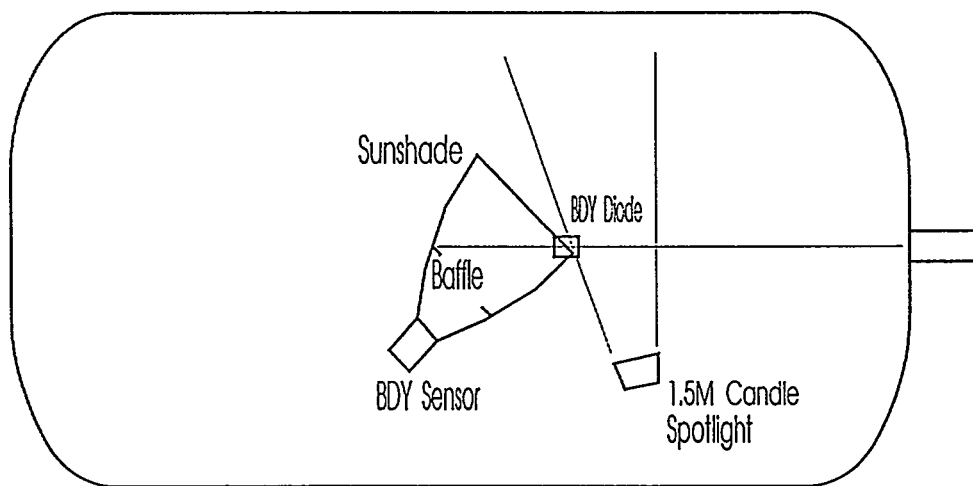


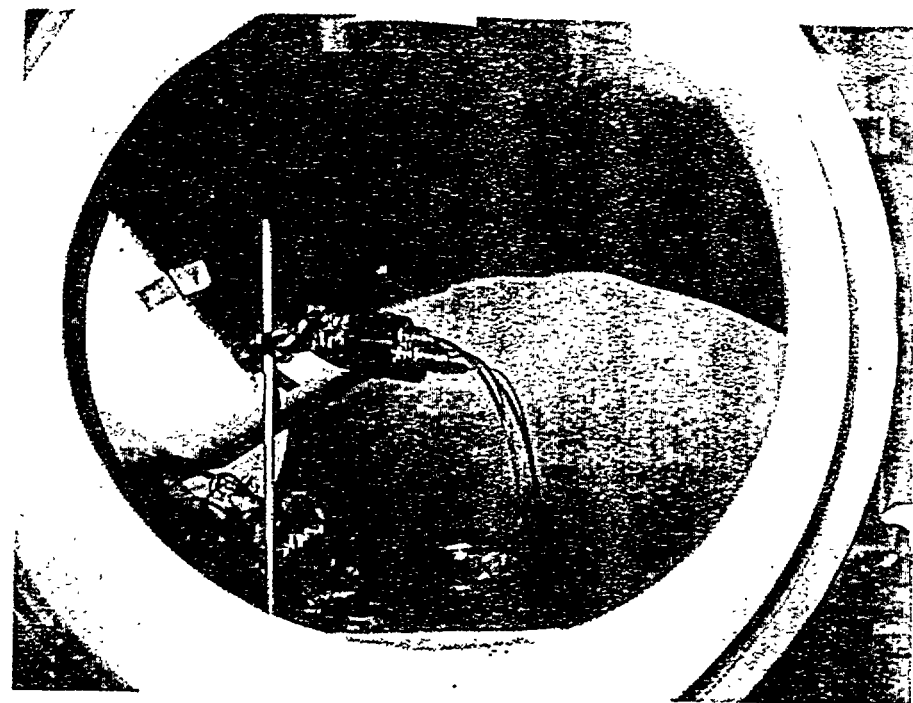
Figure 3. Setup for Line-of-Sight Tests



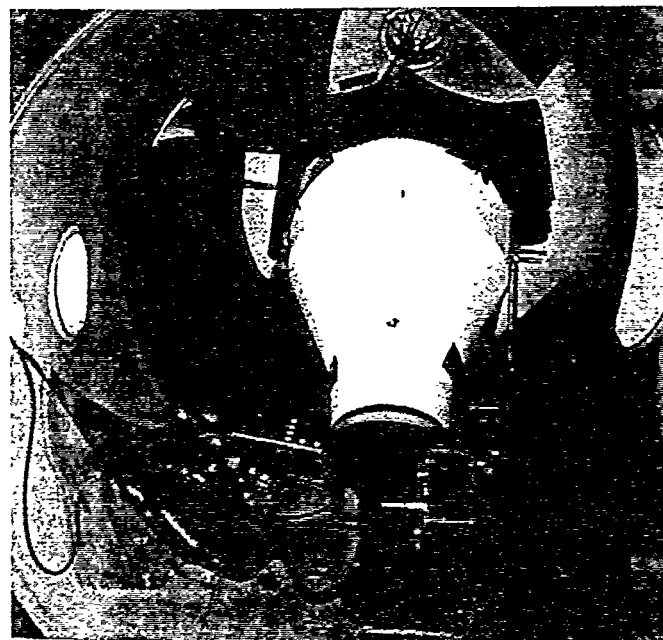
a. schematic

(The BDY Diode is located off axis near the rim of the sunshade and has a line-of-sight view of the impact site.)

Figure 4. Setup for Dark and Illuminated Debris Tests, Continued



b. view from side chamber door



c. view from rear chamber door

Figure 4. Setup for Dark and Illuminated Debris Tests, Concluded

Results

Line-of-Sight Tests

The spacecraft optical sensor response for a line-of-sight impact on a target disk made of sunshade material is shown in Figure 5. The top graph is the optical response in volts measured at the output of the amplifier chain of the sensor electronics. The bottom graph is the same data plotted in "LD Units." The bottom graph is semilog up to 500 microseconds, and then converts to a log-log scale.

The spacecraft optical sensor has a measured risetime and falltime of about 18 microseconds. This time constant is large with respect to the duration of the impact plasma. This suggests that the optical sensor response is an integrated response at the point of the maximum, and that the decay of the response is related to the cooling and geometric dispersion of hot debris.

Local maxima can be seen earlier in time to the maximum of the optical sensor response (to the left of the peak response). This is caused by a small amount of light entering the chamber through the projectile entrance port from the muzzle and from the sabot impacts on the sabot catcher.

Electron micrographs of the craters from two hypervelocity impacts on the target disk are shown in Figure 6. The craters were determined to be the impact sites by the presence of elemental aluminum.

Dark and Illuminated Debris Tests

Two optical detectors were used to instrument the impact tests in darkness and with the sunshade debris illuminated. The spacecraft optical sensor was positioned such that it did not have a line-of-sight view of the impact site inside the sunshade (see Figure 4). A second optical detector, similar to the spacecraft optical sensor, was mounted near the outside rim of the sunshade, and had a line-of-sight view of the impact site inside the sunshade. The purpose of the second sensor was to demonstrate that the optical responses obtained from impacts on a target disk of sunshade material were the same as the optical responses from an impact inside the actual sunshade.

Figure 7 is a comparison of the spacecraft optical sensor response (top graph) with a line-of-sight view of an impact on a target disk of sunshade material (previously shown in Figure 5) with a second optical detector response (bottom graph) with a line-of-sight view of an impact inside the

sunshade. The two responses differ only because of the detector characteristics. The second detector has a 60 microsecond time constant (compared to an 18 microsecond time constant for the spacecraft optical sensor) and the gains obtained from the chain of amplifiers in the signal conditioning electronics are not equivalent. Further, the second optical detector was located about 3 times closer to the impact sight than was the spacecraft optical sensor in the previous tests. Given these differences it is concluded that the light from the impact is not significantly different in characteristics between the two test setups (i.e., the setups shown in Figures 3 and 4).

The spacecraft optical sensor response for an impact in darkness (i.e., spotlight turned off) is shown in Figure 8. In the top graph an inflection occurs after the signal peak. It is believed that this inflection is due to light from the gun entering the chamber through the projectile entrance port and illuminating some sunshade debris. The same data in LD Units is shown in the bottom graph.

The spacecraft optical sensor response for illuminated debris (i.e., spotlight on) is shown in Figure 9. In the top graph a second maximum follows the signal peak and is likely caused by light reflected by the sunshade debris in the field of view of the spacecraft optical sensor. The same data in LD Units is shown in the bottom graph.

A comparison between impacts in darkness (top graph) and illuminated debris (bottom graph) is shown in Figure 10. The effect of illumination of debris in the field of view of spacecraft optical sensor can be seen in the comparison.

Comparison with On-Orbit Data

In Figure 11 the responses from three tests of the spacecraft optical sensor (line-of-sight, impacts in darkness, and illuminated debris) are compared with selected on-orbit signals. The on-orbit signals are shown in the top graphs and the test data from the JSC HIT-F are shown in the bottom graphs.

In the line-of-sight case the selected on-orbit signal compares very well with the test data. Ignoring the response due to muzzle and sabot impact light, the peak response is qualitatively very similar to the on-orbit peak response in the semi-log portion of the graphs. Unfortunately data out to several milliseconds was not acquired for comparison, but the slope of the decay in the log-log portion of the graph suggests that an optical sensor response would have been present up to 10 milliseconds after the impact.

In the case of the impact in darkness the spacecraft optical sensor response is also qualitatively very similar to the selected on-orbit signal.

The spacecraft optical sensor response to illuminated debris is compared with a long duration on-orbit signal (1 second) to suggest that the duration of the signal is determined by how long illuminated debris stays within the field of view of the optical sensor. In the HIT-F tests the field of view is limited by the confines of the test chamber and by the spotlight beam. In the on-orbit case, the cone of the field of view is not truncated and the light scattered by the debris would be detected by the optical sensor until the debris sufficiently disperses.

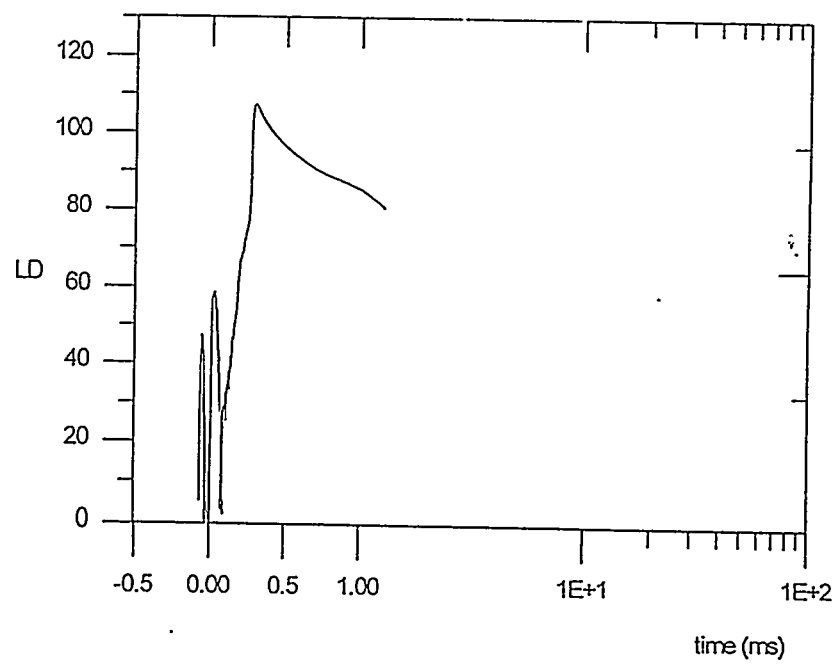
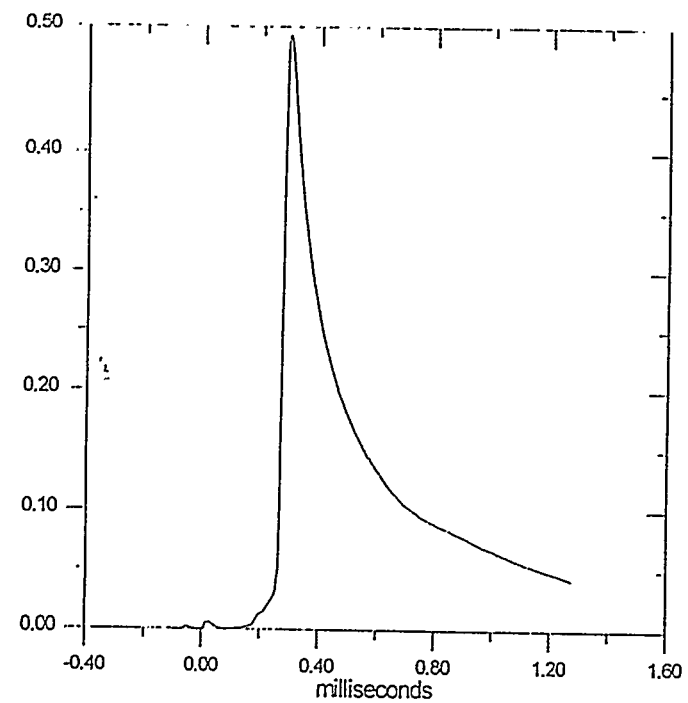


Figure 5. Optical Sensor Response for Line-of-Sight Impact

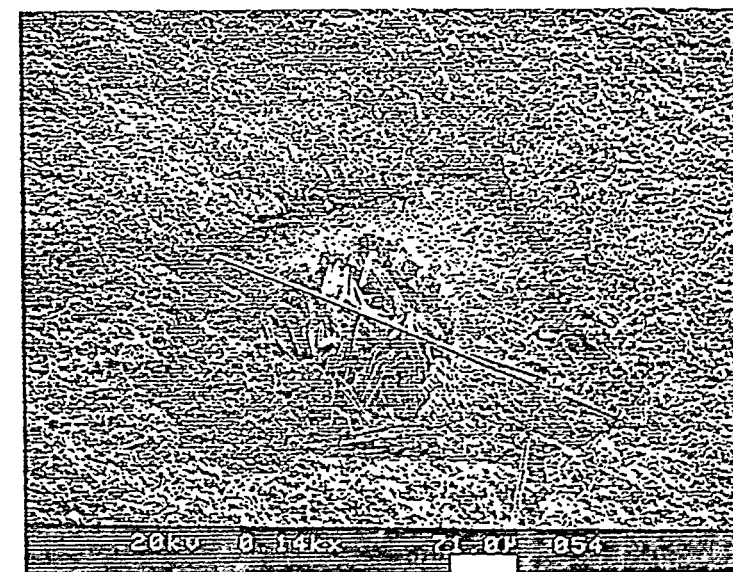
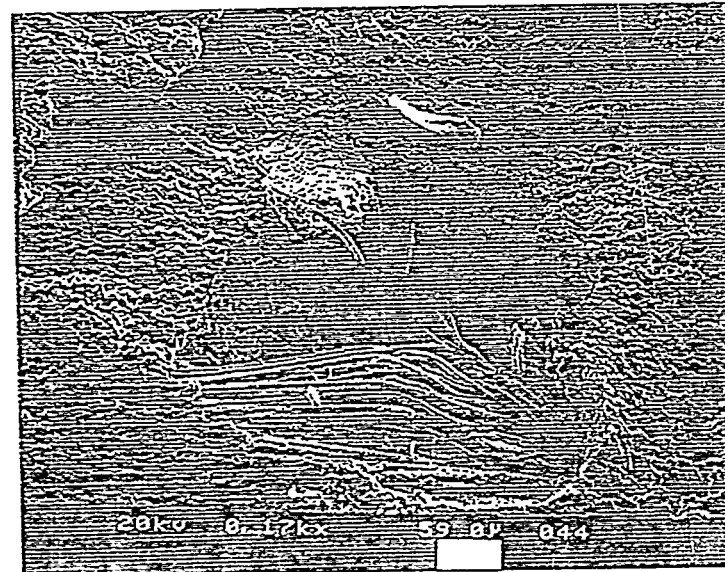
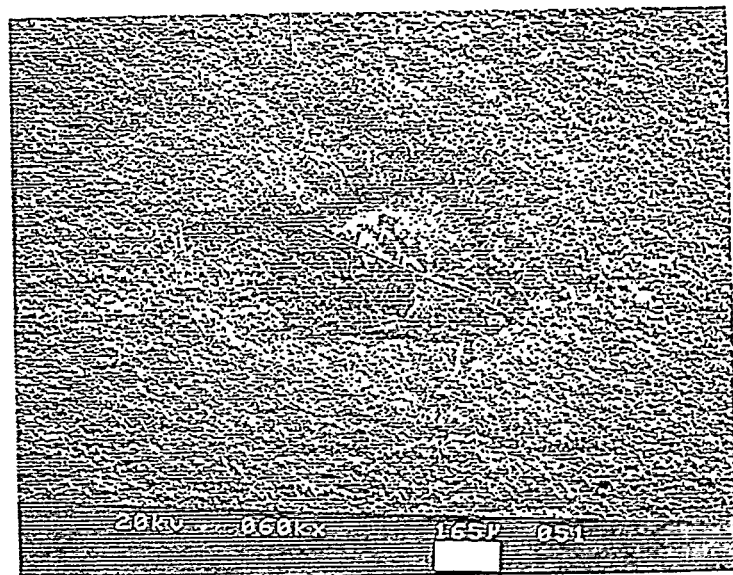
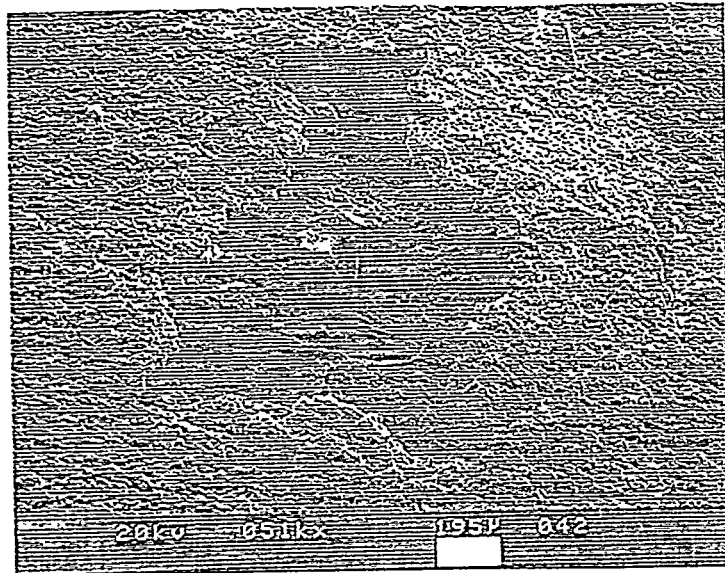
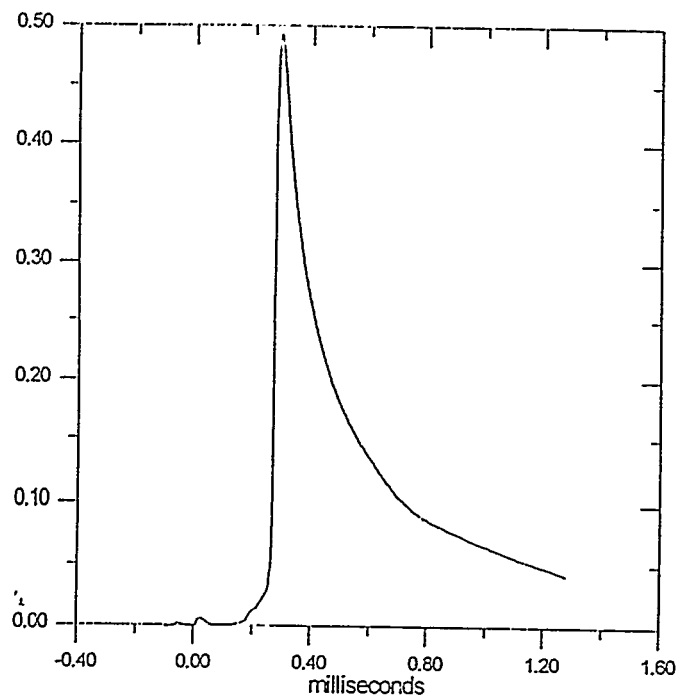
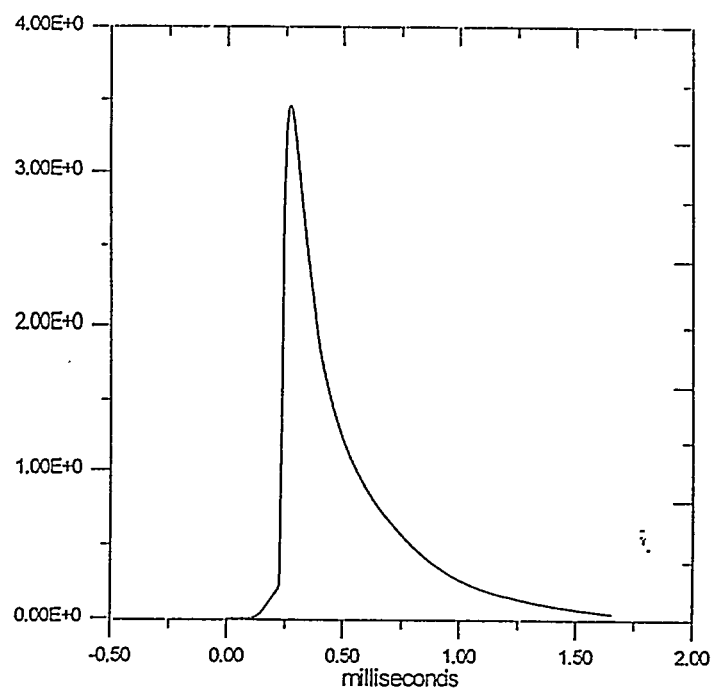


Figure 6. Electron Micrographs of Impact Damage to Sunshade Material
(The deep portion of the impact craters are about 2000 times larger than the diameter of the projectile.)



a. spacecraft optical sensor response from an impact on target disk of sunshade material



b. optical detector response from an impact on sunshade baffle

Figure 7. Comparison of Line-of-Sight Signals

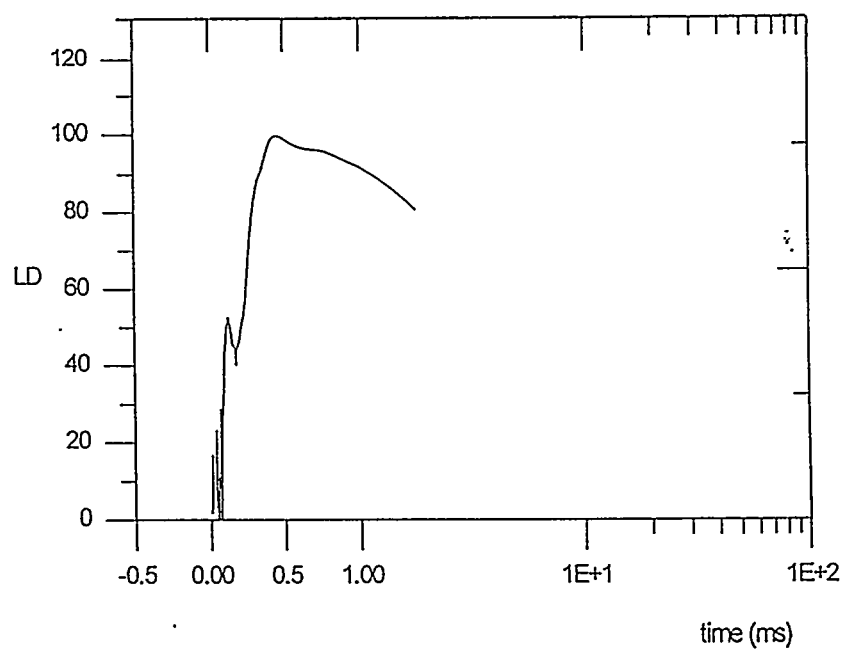
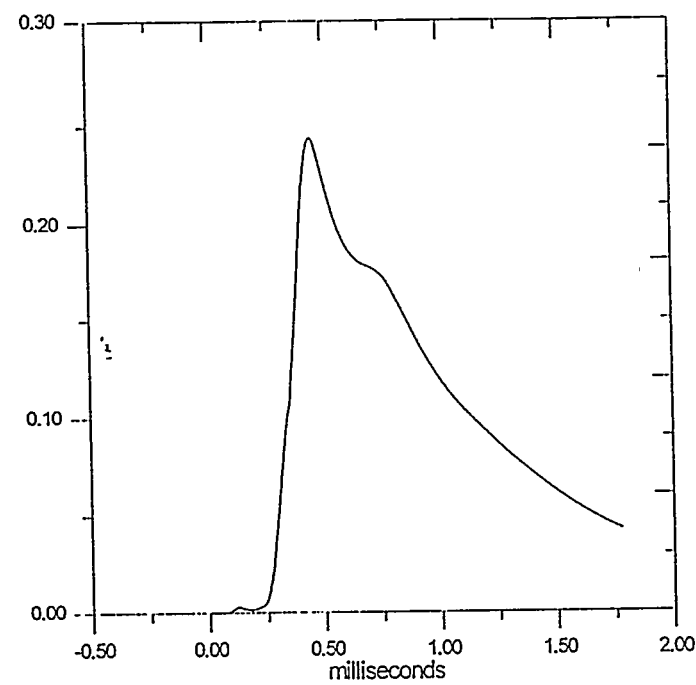


Figure 8. Optical Sensor Response for Impacts in Darkness

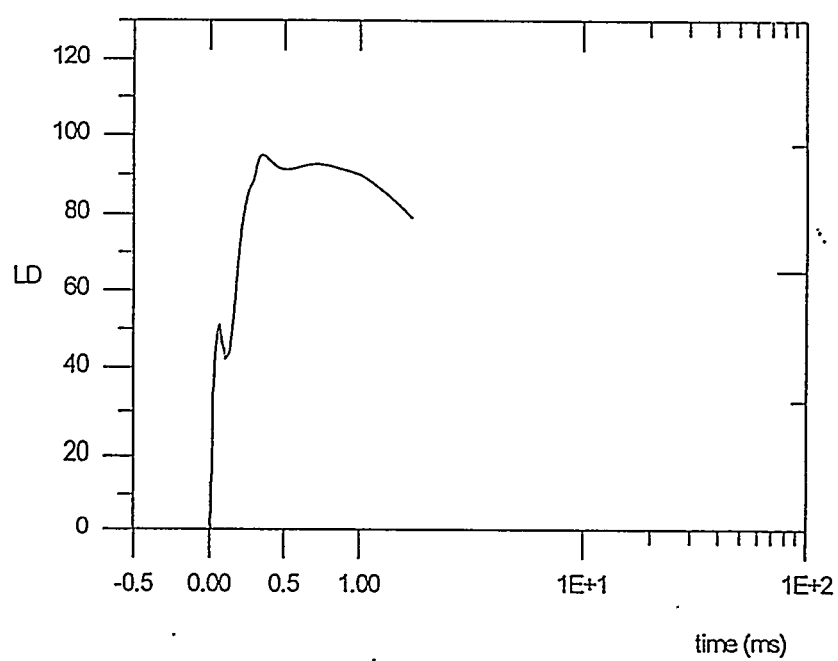
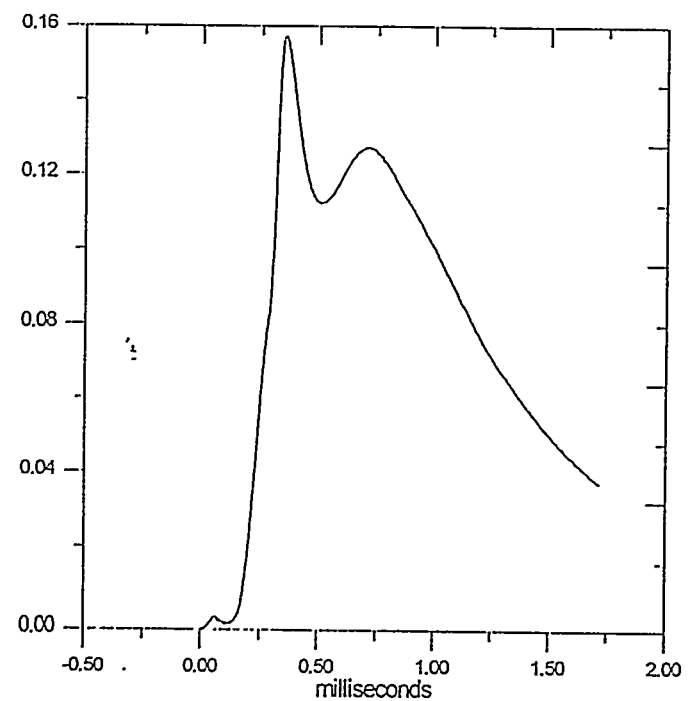
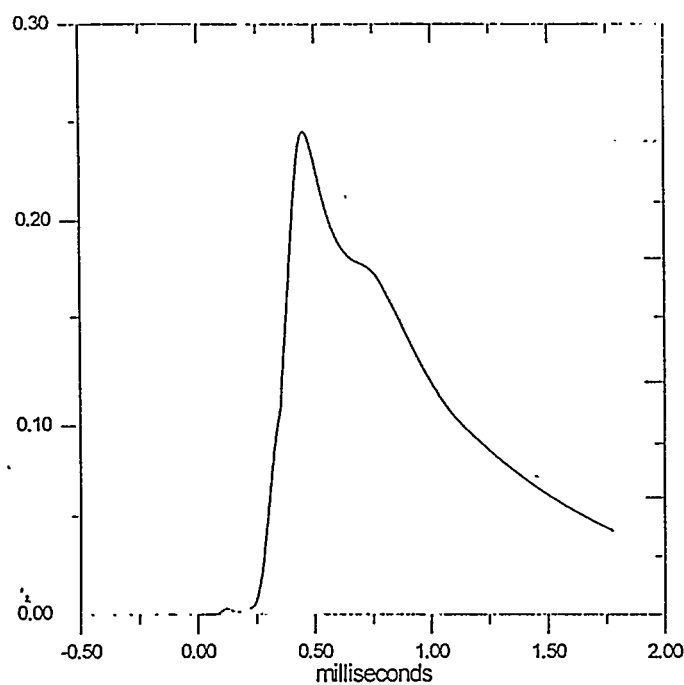
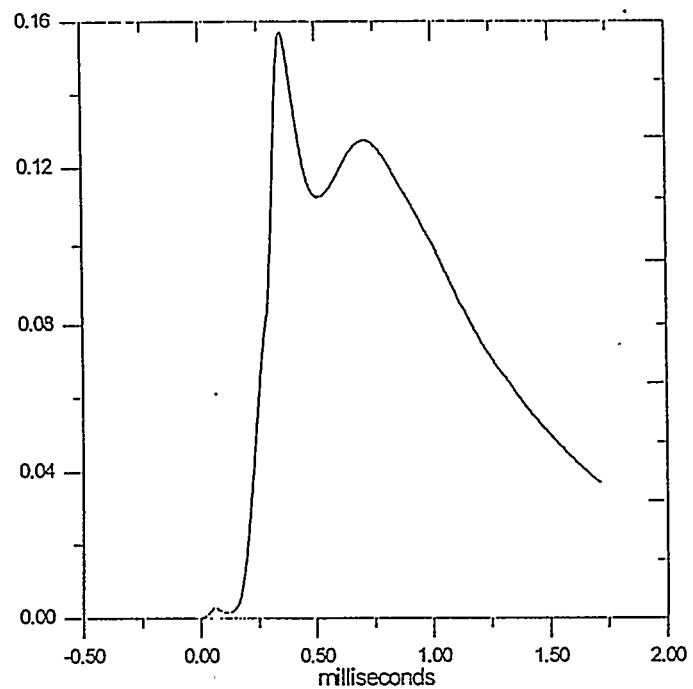


Figure 9. Optical Sensor Response for Illuminated Debris

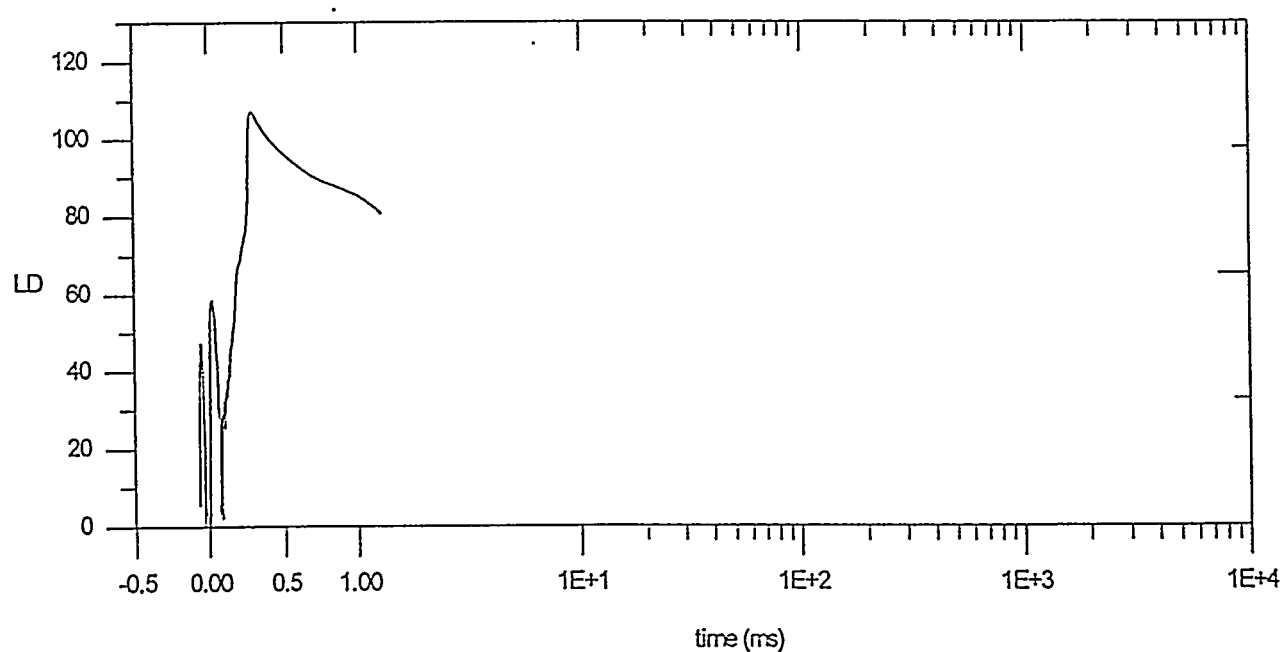
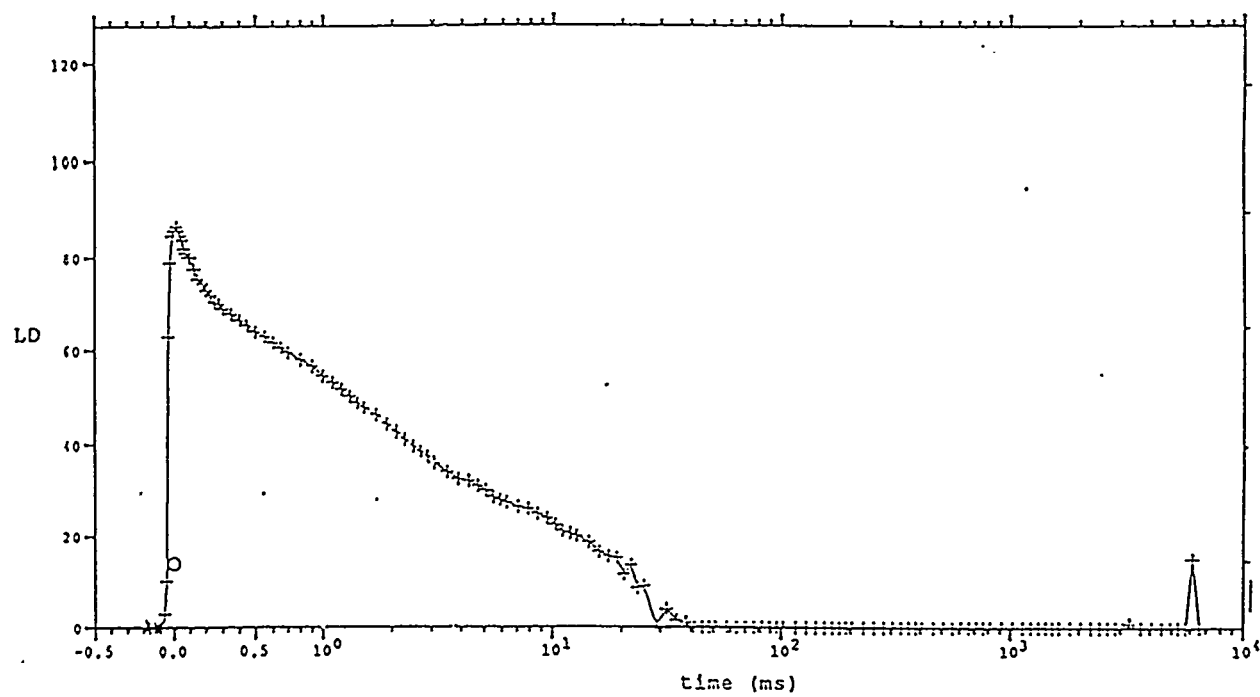


a. test in darkness



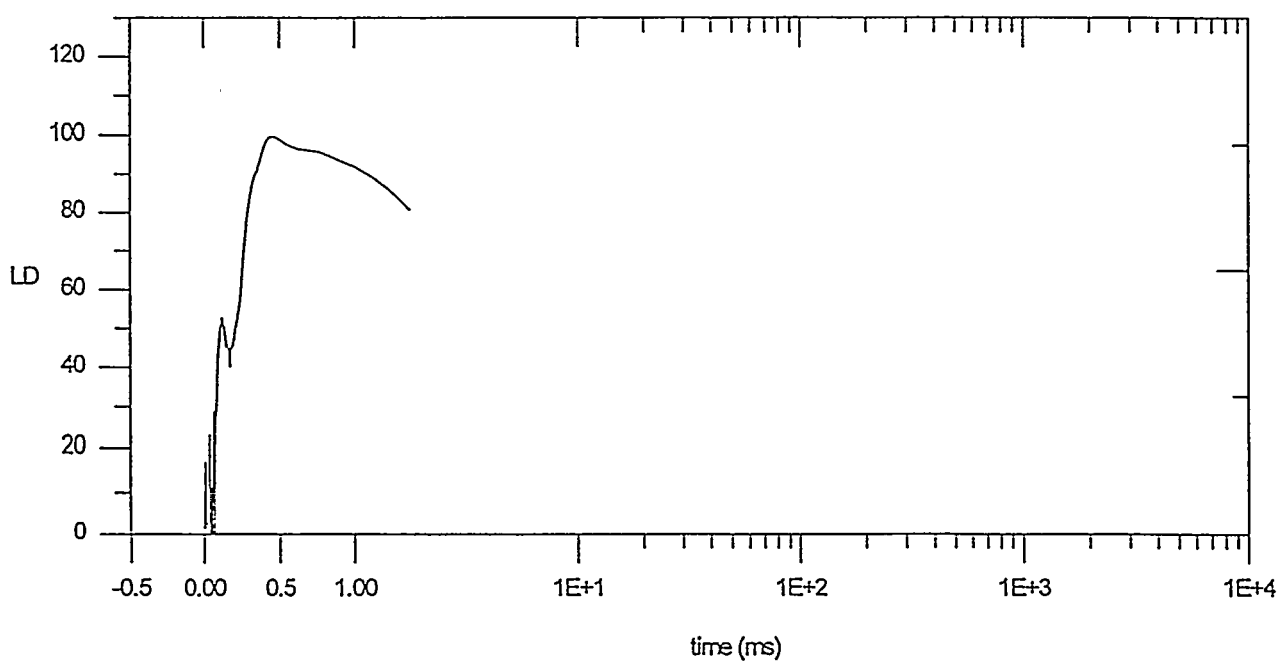
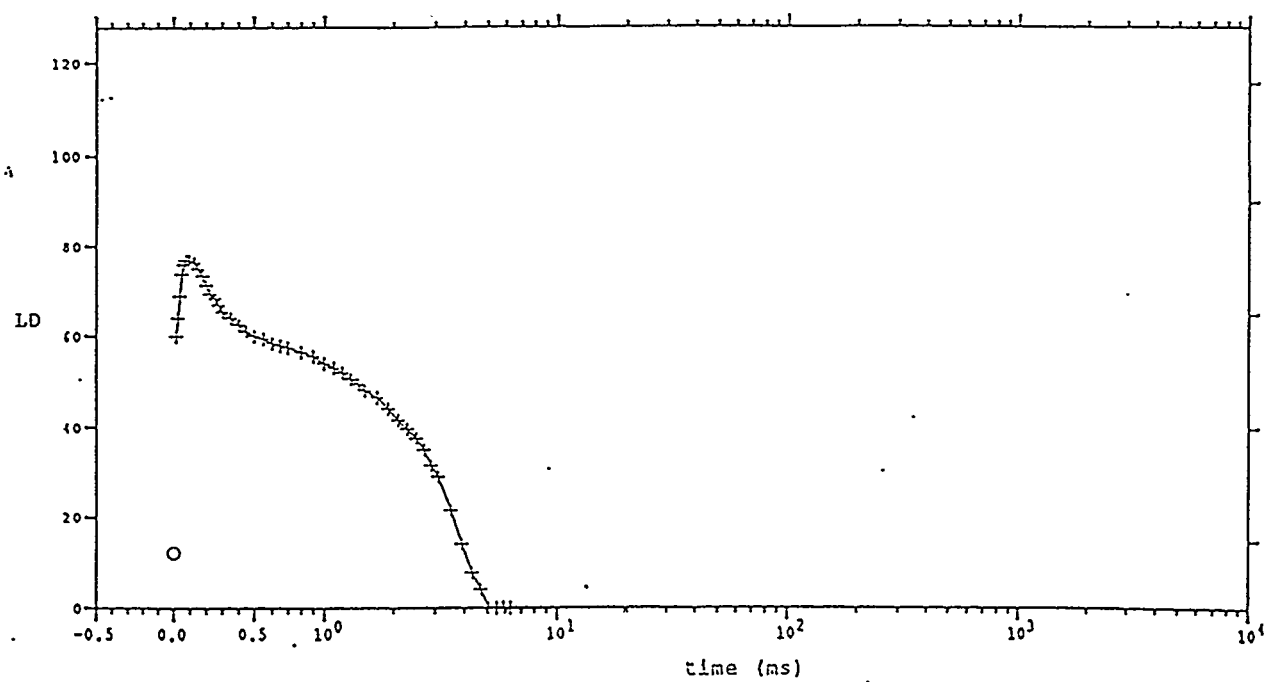
b. debris illuminated

Figure 10. Comparison of Impacts in Darkness and Illuminated Debris Signals



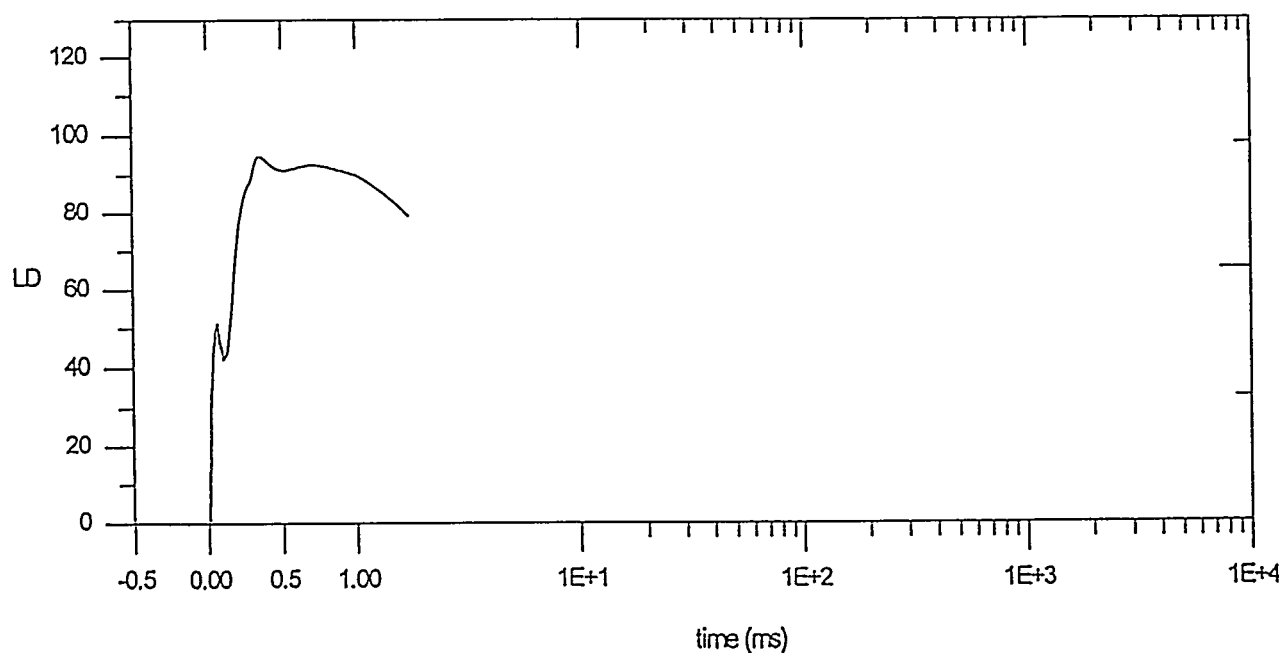
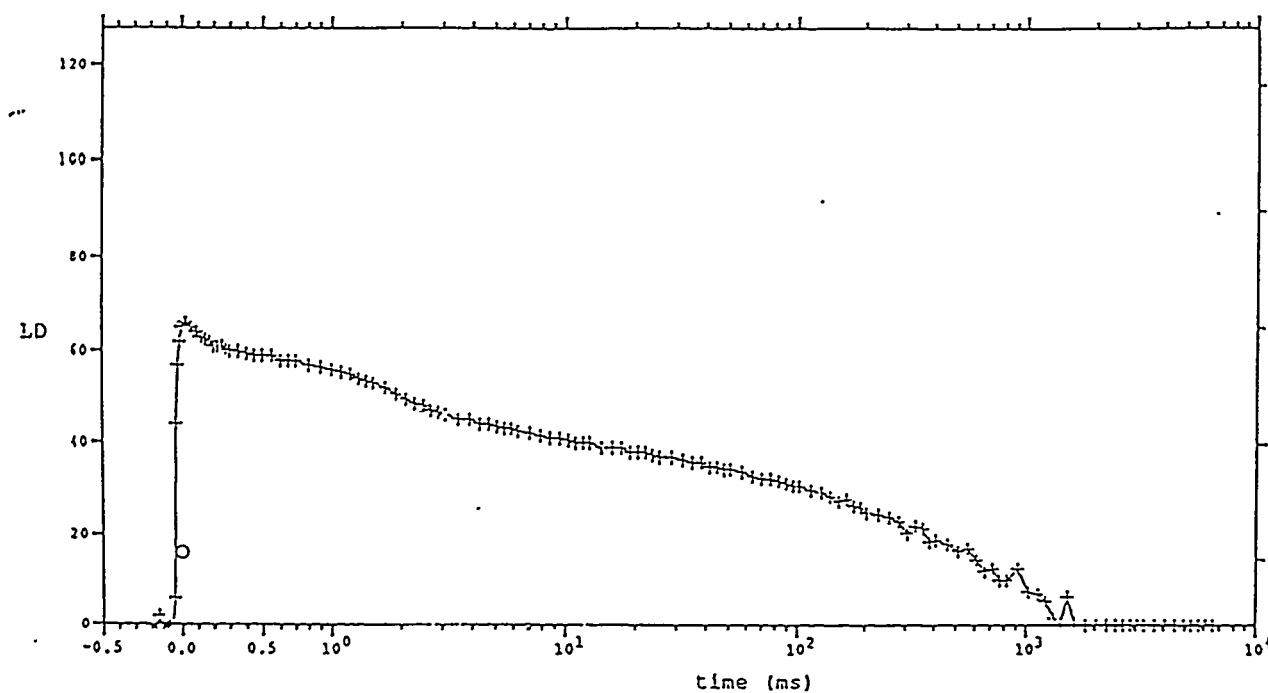
a. line-of-sight

Figure 11. Comparison of Test Results to On-Orbit Signals, Continued



b. impact in darkness

Figure 11. Comparison of Test Results to On-Orbit Signals, Continued



c. illuminated debris

Figure 11. Comparison of Test Results to On-Orbit Signals, Concluded

Conclusions

Hypervelocity impact tests on optical sensors were performed at the Johnson Space Center Hypervelocity Impact Test Facility. A two-stage gas gun was used to propel microgram-size aluminum spheres to velocities of 7.3 km/s. Spacecraft optical sensor responses were recorded from line-of-sight impacts on sunshade material, from impacts inside the sunshade in darkness, and from impacts inside the sunshade with the ejected debris illuminated.

It was observed that all of the spacecraft optical sensor responses resembled on-orbit signals. The test results, however, do not rule out the possibility that other processes may be responsible for the on-orbit signals. Factors not taken into account by this work are:

- The vacuum levels achieved during the tests are not equivalent to the hard vacuum of space. The vacuum has an effect on the formation of the impact plasma and the cooling and dispersion of the impact debris.
- The sunshade of the spacecraft optical sensor is likely to be electrically charged on-orbit. The redistribution of this charge during a hypervelocity impact on the sunshade may affect the optical sensor response.
- Variation in particle velocity, mass and impact site inside the sunshade will affect results.

Abbreviations and Special Terms

BDY Diode	Silicon detector and signal conditioning electronics similar in function but not equivalent to the spacecraft optical sensor
BDY Sensor	Spacecraft optical sensor silicon detector and signal conditioning electronics
JSC HIT-F	Johnson Space Center Hypervelocity Impact Test Facility
LD Units	$LD = 1 + 25 \log_{10} (I/I_0)$, where I is the optical intensity and I_0 is a reference intensity.
Sabot	A thrust-transmitting light-weight carrier that positions a subcaliber projectile in a rifle barrel and is normally discarded when free of the barrel.

Reference

Fox and Wiley, "Hypervelocity Microgram Particle Impact (HIMPI) Study," prepared for AFTAC/DOS, Patrick Air Force Base, Florida, Contract Number F08650-93-D-0050, October 31, 1994.

Appendix

PhotoDetector Response (Excerpts)

J. L. Montoya
November 14, 1994

Introduction

In order to use the Satellite Photodetector (BPD) for measurements at the Johnson Space Center, (JSC), it is necessary to understand the limitations and characteristics of the unit. This can be accomplished by testing its response to repeatable optical signals and by comparing the results to those of other detectors. The units can then be used in the field with a greater understanding of the limitations of each of the instruments.

Optical Pulse Generators

The response performance characteristics of the Satellite Photodetector (BPD), Small Silicon Photodetector SSPD, and the Tk 850 nm and Tk 1300 nm Photodetectors were evaluated using various illumination sources. The units were tested to determine their bandwidth characteristics, i.e., risetime and falltime, their linearity, sensitivity and saturation characteristics.

Square Wave Generator

Using a low power optical square wave generator (operating at 820 nm) with a risetime (and falltime) less than 1 μs , it was determined that the two Tk detectors had the fastest risetimes, less than 1 μs , but had the least sensitivity (volts/watt) to the optical stimulus. The Satellite detector (BPD) had the slowest risetime, approximately 18 μs , and had the highest optical sensitivity. The Small Silicon Photodetector (SSPD), built to accommodate other optical signals, had a faster risetime than the BPD and a greater sensitivity than the either of the Tk detectors. The SSPD has a measured risetime of approximately 1.8 μs and has a sensitivity between that of the other two detectors.

Strobe Light

A Xenon strobe light was used to characterize the detectors at a high light level and with a wide spectral content source relative to the optical square wave generator. Figure 1 shows that the response of the BPD compared to the response of the SSPD detector. The limited risetime of the BPD (18 μs) causes an apparent time shift in the peak of the

waveform, and causes the decay time to appear longer. This slower response is possibly a result of the larger detector surface area, and consequently higher capacitance, of the detector in the BPD as compared to the SSPD. From a visual inspection of the detectors, the active area of the BPD is estimated to be about 1856 mm^2 , while the area of the SPD is about 78 mm^2 . This ratio of the areas is 23:1, however, a direct comparison of the capacitances depends also on the thickness of the detector substrate, an unknown factor.

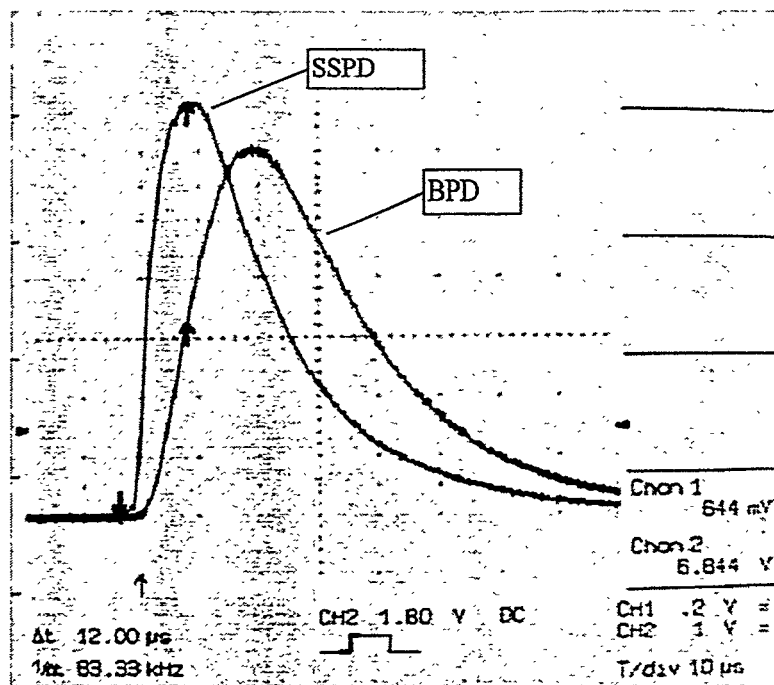


Figure 1. Comparison of the BPD and SSPD to Strobe.

Since both detectors have similar spectral sensitivities, it is unlikely that significant risetime differences are due to the spectral response characteristics. The BPD, including optics, operates over a spectral bandwidth of 340 nm to 1200 nm while the SSPD operates from 400 nm to a maximum of 1100 nm .

Shown in Figure 2 is the response of the SSPD and the Tk 850 nm sensors to the same strobe light signal. The Tk 850 nm sensor has a spectral bandwidth extending from approximately 400 nm to 1050 nm and has a measured risetime of less than 1 μs . From the photo, it is apparent that both the SSPD and the Tk 850 closely follow the optical signal, with the Tk having a slightly better risetime. However, the Tk PhotoDetector is several orders of magnitude less sensitive than the SSPD and must be located close to the source before a reasonable signal-to-noise ratio can be achieved.

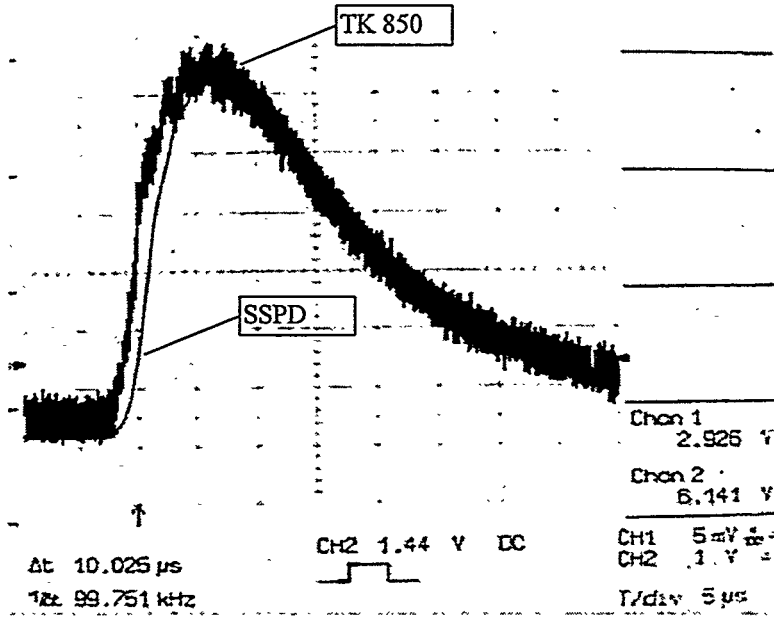


Figure 2. Comparison of SSPD and Tk to Strobe.

A similar test conducted with the Tk 1300 nm sensor showed similar results to the test with the Tk 850 nm . Although the Tk 1300 nm has a spectral bandwidth extending from 950 nm to about 1700 nm , widely different from the other detectors, the results were very similar to the SSPD and to the 850 nm detector. The Tk 1300 nm and the SSPD detector risetimes and falltimes compared favorably, but the Tk had a sensitivity level several orders of magnitude lower than the SSPD.

A better comparison of the detectors can be accomplished through the use of a high intensity, relatively slow rising optical signal. This allows the BPD to track the rise time of the signal and also produces enough light to be sensed by the Tk detectors. Shown in Figure 3 is a normalized comparison of the BPD and SSPD detectors for a flashbulb fired from a 6 volt lantern battery.

The slow risetime (15 ms) allows the BPD

detector to easily track the optical signal. With this source, the BPD and the SSPD track the waveform identically. This same test conducted with the two Tk probes compared to the SSPD produced the nearly identical results showing that the four detectors will track each other for a relatively slow signal. The absolute amplitude of the signal from the detectors however, will depend on the spectral content of the source and the distance between the source and the detector.

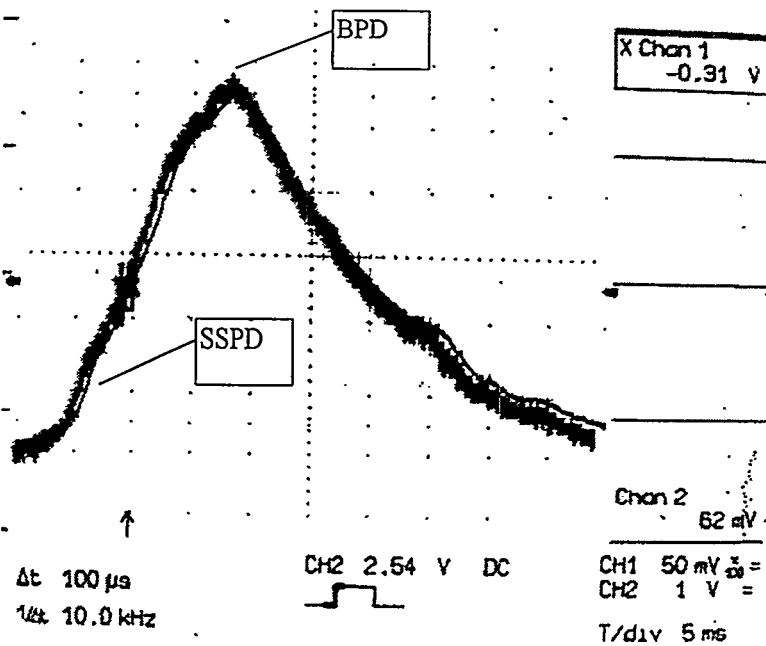


Figure 3. BPD and SPD with a Flashbulb Source

Conclusions on the Relative Performance of the Detectors

Although the Satellite PhotoDetector (BPD) has the highest sensitivity to light, it also has the lowest bandwidth (18 μs when compared to the two Tk detectors and to the Small Silicon PhotoDetector (SSPD). Tests with a strobe light showed that although the BPD detector could not follow the risetime of the optical pulse, the recorded signature could be used for testing the performance of the detectors and instrumentation in a field application.

Addendum

Tests not described above, showed that the BPD Diode had a risetime of approximately 60 μ s with a comparable falltime. The output of this unit however, when pulsed with a flashlamp, followed the waveform exactly as did the other detectors.